

SIMULATION AND DESIGN OF TUBULAR ELECTRON STRING ION SOURCE

D. E. Donets, E. D. Donets, E. E. Donets, V. M. Drobin, A. V. Shabunov, Yu. A. Shishov, V. B. Shutov, E. M. Syresin*, Joint Institute for Nuclear Research, Dubna, Russia

A.E. Dubinov, R. M. Garipov, I.V. Makarov, Russian Federal Nuclear Center “All-Russian Institute of Experimental Physics”, Sarov, Russia.

Abstract

The so-called reflex mode of Electron String Ion Source (ESIS) operation has been under intense study, both experimental and theoretical at JINR during the last decade. The idea of using a tubular electron string ion source (TESIS) has been put forward recently to obtain 1-2 orders of magnitude increase in the ion output as compared with ESIS. The project is aimed at creating TESIS and studying an electron string in the tubular geometry. The new tubular source with a superconducting solenoid up to 5 T should be constructed in 2010.

The method of the off-axis TESIS ion extraction will be used to get TESIS beam emittance comparable with ESIS emittance. It is expected that this new TESIS (Krión T1) will meet all rigid conceptual and technological requirements and should provide an ion output approaching 10 mA of Ar¹⁶⁺ ions in the pulse mode and about 10 μA of Ar¹⁶⁺ ions in the average current mode.

Analytical, numerical study of the tubular electron strings and the design of the TESIS construction are given in this report. The experiments with quasi tubular electron beams performed on the modified ESIS Krión 2 are also discussed there.

TUBULAR ELECTRON STRING ION SOURCE

The Electron String Ion Source is based on a specially designed electron gun and an electron reflector that allows multiple uses of beam electrons [1-3]. At some conditions the electron string is formed with about few hundreds reflections for each electron. The electron string can be used for production of highly charged ions similarly to beam electrons. The interest in the ESIS mode was motivated by the attractive possibility of decreasing the electron beam power by a factor of 100 preserving simultaneously the same ion yield. The Krión-2 ESIS has been used successfully at the injection complex of JINR synchrotron Nuclotron for production of highly charged ion beams: Ar¹⁶⁺ - 200 μA, Fe²⁴⁺ - 150 μA in 8μs pulses (see Table 1) [3].

The idea of using TESIS was proposed in [4] to obtain a considerable increase of ion outputs (Table 1) in comparison with the ESIS and simultaneously a small ion beam emittance, usually provided by ESIS. The method of the off-axis TESIS ion extraction was proposed in [4-5] to get beam emittance comparable with ESIS one.

In fact, the number of produced ions is proportional to the number of the stored electrons and for a given source

length it is proportional to the beam cross-section area. The ratio of the stored electrons/ions in the tubular source N_{TESIS} and in the solid cylindrical beam N_{ESIS} of the same length is $N_{TESIS}/N_{ESIS} \approx 4r/a \approx 25 \div 50$, where a is the radial electron beam thickness and r is the main radius for the tubular electron beam. Second crucial point is that the use of tubular geometry of drift tube structure allows avoiding the virtual cathode formation for the corresponding amount of accumulated electrons in comparison to the cylindrical drift tube structure.

It was found experimentally [1-3] that the maximum number of electrons N_e accumulated in a linear string was proportional to a confined magnetic field B to the third power:

$$N_e = \kappa B^3 \quad (1)$$

An increase in the magnetic field from 3 T in Krión-2 to 5 T in Krión-T1 permits 5 times increases of the ion yield.

Table 1. Parameters of Electron String Ion Sources

Ion source	Krión-2	TESIS
Electron energy, keV	3÷5	3÷5
Number of stored electrons	$5 \cdot 10^{10}$	$3 \cdot 10^{12}$
Magnetic field, T	3	5
Ion current, mA	0.15	10
Pulse duration, μs	$8 \div \infty$	$8 \div \infty$
Maximal number of Ar ¹⁶⁺ extracted ions	$5 \cdot 10^8$	$3 \cdot 10^{10}$
Ion extraction frequency, Hz	1	5
Average ion current, mA	0.15	10

NOTES ON TUBULAR ELECTRON STRING EXPECTED PARAMETERS

The density of the tubular electron string is determined by the initial injected electron current density and by the time of the electron escape from the ion source. It is reasonable to consider electron escape rate based on test electron propagation properties ignoring for a while corresponding contributions from collective effects. The escape of the stored electrons depends on an electron elastic scattering angle α_{gun} , which is produced at a reflection of the electrons from gun and collector potential barriers. As a rule, the electron gun and reflector are situated in the fringe magnetic field with $B_{min} = B/20$, where B is a value of the magnetic field in the uniform

region. The scattering angle α_{gun} strongly depends on the magnetic field in the gun region $\alpha_{\text{gun}} \cong (r_c/d) \cdot (\rho/d) \cong 10$ mrad, where $r_c=1$ mm is the tubular cathode emitter width, $d=10$ mm is the cathode-anode gap, $\rho=v/\omega=1$ mm is the Larmor radius in the gun or collector magnetic field $B_{\text{min}}=0.25$ T, v is the total electron velocity, $\omega=eB_{\text{min}}/mc$ is the cyclotron frequency in the magnetic field B_{min} , e and m are the electron charge and mass, c is the velocity of light. The gun/collector electron scattering angle is increased to $\alpha=\alpha_{\text{gun}} \cdot R^{1/2} \cong 50$ mrad as electron penetrates into the uniform magnetic field region with $B=5$ T, where $R=B/B_{\text{min}}=20$ is magnetic trap ratio.

There are two evident channels of the electron escape in this scenario without collective effects. Main part of the stored electrons escape the ion source due to the transverse diffusion, caused by the mentioned scattering at gun/reflector regions. The other part of the stored electrons could be captured after $N_{\text{os}} \cong 1/4\alpha^2 \cong 100 \div 300$ oscillations in the magnetic traps formed between edges of solenoid and the gun or collector potential barriers due to electrons entering into the “cone loss” functional space.

The number of string electrons stored in the ion confinement region could be estimated as

$$N_c = (I_e \cdot L / v \cdot e) \cdot (1/4\alpha^2) \cong 3 \cdot 10^{12} \quad (2)$$

where $I_e=0.2$ is the electron injection current, $L=1.0$ m is the setup length. Reduction of the confining magnetic field B leads to the corresponding reduction of the stored electrons (2) because of an increase of the scattering angle α . In the high magnetic field the radial half-width of a tubular beam $a/2=110 \mu\text{m}$ is twice as large as the Larmor radius $\rho_B=50 \mu\text{m}$ calculated at full electron energy and B . In this case the electron escape is realized mainly due to capture in the “cone loss”.

The main favourable effect of dense electron string formation is related to energy spread $\Delta E/E_0$ of the stored electrons. The energy spread was experimentally observed with linear electron string and it is caused by the collective interaction of the stored electrons. The large electron energy spread leads to strong reduction of the space charge effects in the gun region at a high string density. The oscillating electrons with low energy practically do not have influence on the operation of the gun since they are reflected from the potential barrier far enough from the emitter surface. The maximal density of stored string electrons in the gun region essentially depends on the electron energy spread (Figure 1). For example, the density of string electrons n_0 in the gun region increases by the factor $k=n_0/n_{b0}=11.5$ at $\Delta E/E_0=0.3$ (Figure 1) compared with nominal Child-Langmuir density n_{b0} . The gun perveance $P_{\text{g-st}}$ for a tubular string with a wide electron energy spread is also k times larger $P_{\text{g-st}}=kP_{\text{g}}$, than the gun perveance related to the Child-Langmuir low $I_{b0}=P_{\text{g}}U_{3/2}$. At energy spread $\Delta E/E_0 \cong 1$ string density increases to $n_0/n_{b0}=27$, however the yield of highly charged ions reduces because of a decrease of the ionization cross section caused by the low energy string

electrons. These electrons make a small contribution to the deep ionization of highly charged ions. The yield of highly charged ions reduces at a large electron energy spread $\Delta E/E_0 > J/(2J+e\Delta U) \cong 0.3-0.4$, where $E_0=5$ keV is the electron energy, it corresponds to $E_0 \cong 2J+e\Delta U$ at the optimal ion ionization, $e\Delta U \cong 1.5$ keV is the kinetic electron energy reduction related to the string space charge effects, J is the ionization potential of the highly charged ions, $J \cong 1-2$ keV for ions like Ar^{16+} and Fe^{24+} . There is an optimal electron energy spread for production of dense string at which an intensive highly charged ion beam is formed. Below in simulation we consider the uniform energy distribution function in the interval of $2/3E_0 < E < E_0$ typical of the experiments with the linear electron strings [1-3]. In fact, it was experimentally observed that there are some amounts of string electrons with kinetic energy larger than injection energy; however, presence of this high energy electron tail works in the enhancement side of the given estimations.

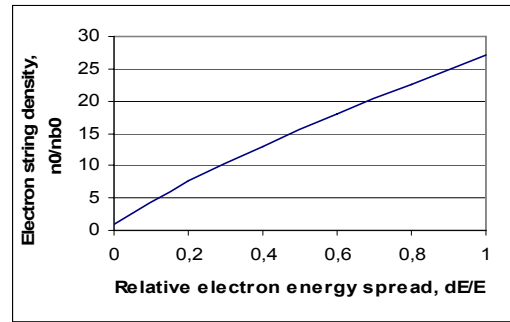


Figure 1. Ratio of string electron density to the Child-Langmuir density n_{b0} versus the electron energy spread.

The tubular geometry of drift tube structure permits a 25÷50 time's increase in number of the stored string electrons comparing to the linear one. The drift chamber perveance P_{ch} should be larger the gun perveance $P_{\text{g-st}}$ for tubular string with a wide electron energy spread $P_{\text{ch}} > P_{\text{g-st}}$ to avoid virtual cathode formation. The virtual cathode formation leads with necessity to formation of a low energy electrons and therefore to reduction of yield of the highly charged ions. The number of stored electrons in a high intensity tubular string is

$$N_c = (\Delta U_{\text{an}} \cdot L / e) \cdot 2r / h_{\text{ap}} \cong (k \cdot I_{b0} / e) \cdot (L / v) \cong 4 \cdot 10^{12} \quad (3)$$

at $P_{\text{ch}} > P_{\text{g-st}}$, here $k \cdot I_{b0}/2$ is the current of string electrons propagating in one longitudinal direction, $I_{b0}=1.9$ A is the beam current corresponding to the Child-Langmuir low, $U=5$ kV is the cathode-anode accelerating voltage, $k=11.5$ is the gain in the string density for electrons with the energy spread $\Delta E/E_0=0.3$, $r=8.2$ mm is the radius of central beam line in the high magnetic field region, $h_{\text{ap}}=1$ mm is the minimal electron string radial aperture in the uniform magnetic field B , ΔU_{an} is the potential inside of anode diaphragm related to electron string space charge, $\Delta U_{\text{an}}=U/[1+(d^2/1.3Rh_{\text{ap}}a) \cdot (1+47\alpha^2)]$. The value $d^2/(1.3Rh_{\text{ap}}a)=P_{\text{an}}/P_{\text{g-st}}$ defines a ratio of the anode

diaphragm perveance P_{an} to the gun perveance $P_{g-st.}$, where $P_{an}/P_{ch} = h/h_{ap} = 3$, $h = 3$ mm is the radial gap between the coaxial tubular drift chambers in the ion confinement region. The coefficient $1 + 47\alpha^2$ is related to the contribution of the electron scattering effects to formation of a high intensive tubular string. At saturation of the tubular string capacitance the number of stored electrons N_e (3) has more slow dependence on the electron scattering angle α and the magnetic field B compared with (2) and experimental dates (1). The potential of the tubular string ΔU in the ion confinement region is defined by the equation $\Delta U \cdot (U - \Delta U)^{1/2} = U^{1/2} \cdot \Delta U_{an} \cdot (h/h_{ap})$ at $h \gg h_{ap}$. The virtual cathode is formed here at $\Delta U = 2/3U$. To avoid creation of virtual cathode in the high magnetic field region the potential inside anode diaphragm ΔU_{an} should be lower than $\Delta U_{an} < U \cdot (2h_{ap}) / (3^{3/2}h) = 0.13U$ or the cathode-anode gap should be larger than $d > d_0 = \{(1.3Rha/2) \cdot (3^{3/2} - 2h_{ap}/h)\}^{1/2} = 6$ mm. The virtual cathode is formed at $d < d_0$ ($P_{ch} < P_{g-s}$) and number of stored string electrons is equal to

$$N_{max} = (2U \cdot L / 3e) \cdot 2\pi / h = 1,5 \cdot 10^{13} \quad (4)$$

At a high electron scattering angle α (low magnetic field) the electron string is formed with intensity (2). At a high magnetic field and $P_{ch} > P_{g-s}$ the maximum number of string electrons is defined by (3). This regime corresponds to formation of a high intensive tubular string without creation of virtual cathode. In opposite case $P_{ch} < P_{g-s}$ (4) the virtual cathode is formed in the ion source, as result, the string electrons have the large energy spread $\Delta E/E_0 \cong 1$, which leads to reduction of yield of the highly charged ions.

EXPERIMENTS WITH QUASI-TUBULAR ELECTRON BEAMS

Experiments with quasi-tubular electron beams were performed on the modified ion source Krion-2. Eight special electron guns were installed (Figure 2) on equal radial distance but at different azimuthal angles along the circle in fringe magnetic field region ($1/20 B$). Each such IrCr emitter of 1 mm diameter injected a separate pencil beam towards uniform magnetic field region where tubular drift tube structure has been installed as well.

Annular repeller ring was installed at opposite side of the source mirror symmetrically to the gun geometry in respect to the center of the solenoid. However only 4 holes in repeller were produced and 4 corresponding electron collectors behind them were installed.

The quasi-tubular electron beam (Figure 3) has been formed by those 8 pencil azimuthally distinct electron emitters. We planned to fulfil whole space between distinct pencil beams in the azimuthal direction due to azimuthal electron drift motion. Special electrodes were

installed in the modified Krion-2 source to produce radial electric field leading to the azimuthal electron drift motion in the longitudinal uniform magnetic field.

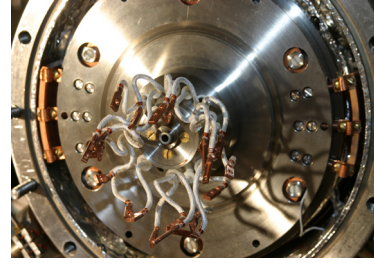


Figure 2. Back side of quasi-tubular electron gun assembly with 8 distinct electron emitters, installed at various azimuthal angles.

The experiments in such set-up allowed to investigate dynamics of separate beams as well as to check effects related to the azimuthal asymmetry of the solenoid magnetic field and the azimuthal imperfection of the ion source mechanical constriction. At variation of the radial electric field the pencil beam from each gun was able to enter the two nearest collectors placed at different azimuthal angles at opposite side of the source (Figure 3).

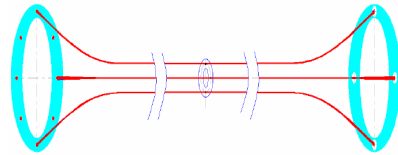


Figure 3. Distinct electron beams and their azimuthal rotation by the applied radial electric field.

The experimental results related to transportation of the pencil electron beams are given in Fig 4. When the pencil electron beam is accepted by the collector the repeller current is became equal to zero. At variation of the radial electric field one can provide condition when the pencil electron beam is turned on azimuthal angle 90° (Figure 3) by the drift electrodes and therefore it is collected by second collector (second peak in the Fig 4a).

The electron beam widths are given in Figure 4b for first and second collectors. They are equal to 4.5 mm in the first collector and 5.2 mm in the second one. The increase in the beam width in the second collector is due to the action of the large radial electric field of the drift electrodes together with the electron angle and energy spreads. The collector current of the pencil electron beam depends on the number of the reflections from repeller electrode and cathode. The collector current without reflection is 20% larger than its value after two reflections from the repeller electrode and the cathode.

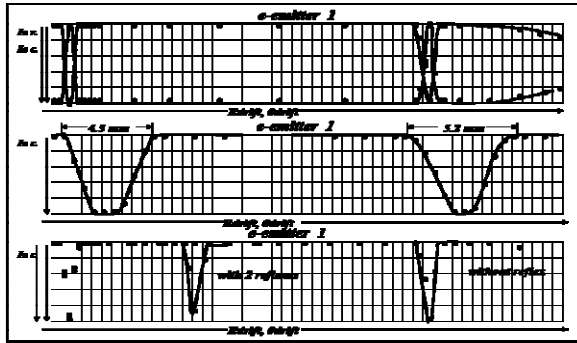


Figure 4. Dependences of collector and repeller currents on the radial electric field.

The performed experiments permit to investigate the azimuthal symmetry of the longitudinal magnetic field and to define a parallelism of the magnetic field axis and the setup axis and showed, that the symmetry in the Krion-2 is not perfect .

DESIGN OF TESIS KRION T1

The tubular electron string ion source [6] (Figure5) consists cryomagnetic, electron-optical, ion-optical and vacuum systems, power supplies, diagnostic and control electronics. The parameters of the superconducting solenoid are given in the Table.2. The superconducting solenoid is fixed by two supports on the vacuum chamber. The cryocooler head is placed at the edge of the cryostat part. The current loads, thermal shielding, superconducting keys, cooled diodes and resistors are placed between the cryocooler and the solenoid. The thermal shielding is connected with the first cryocooler section at the temperature of 4.2 K. The power of the first cryocooler section is 1.5 W. The temperature of the second cryocooler section is of 40 K. The electron gun, reflection electrodes and other elements have temperature from room to cathode temperature.

Ultrahigh vacuum of 10^{-9} – 10^{-10} Pa is the a feature of the tubular electron string ion source. This vacuum should be provided in the space between the internal and external drift tubes. The choice of the vacuum system design is dictated by a small diameter of drift tubes (internal diameter is 0.9 cm, external one is 1.5 cm) which are 120 cm long. The cryo-pumping conception was adopted for TESIS. The external pumping provides preliminary pressure of 10^{-4} Pa and then an ultrahigh vacuum is achieved at cryosorption of surfaces cooled to temperatures of 4.2 K and 40 K. The external drift tube is cooled to 4.2 K, which permits its internal surface to work as a cryopanel on which all gases are frozen (except He, H₂). The internal drift tube is connected to the cryocooler section at 40 K. The surface of the internal drift tube works also as a cryopanel with a smaller sorption efficiency as compared with the external one. Different gases except He, H₂ are also frozen here. Some problems can be appeared at pumping of hydrogen.

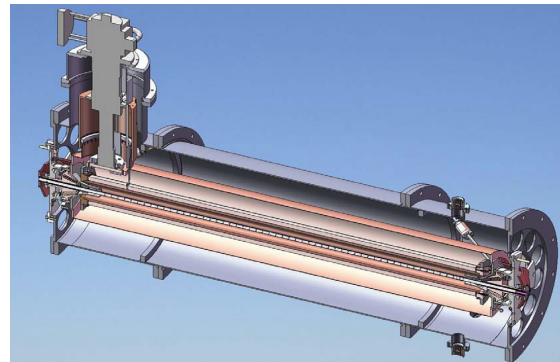


Figure 5 General view of the TESIS.

Table 2. Parameters of Magnetic System

Parameter	Value
Internal solenoid diameter, mm	70
External solenoid diameter, mm	101
Solenoid length, m	1.2
Maximal current, A	95.22
Number of windings per layer	2263
Number of layers	22
Total number of windings	49786
Thickness layer, mm	0.63
Current density, j/mm ²	285.1
Maximal field, T	5.0
Fr, kG/radian	2.46×10^4
$2 \times \pi \times Fz$, kG	5.68×10^3
Induction, Gn	14
Stored energy, kJ	63
Cooled mass at 4.2 K, kg	~ 50

It is connected with high outgasing of hot gun surfaces and the anode reflector. A high level of outgasing is usually realized at the initial work stage and it essentially decreases with increasing operation time. The external pumping is provided only for initial operation time. As the gun and the reflector electrodes are placed near the pumps on both edges of the setup and this reduces the problem at initial pumping of hot surfaces.

Based on the computer simulation we designed the electron-optical (Figure6) and ion-optical systems (Figure7). The electron gun has three electrodes. The diameter of the cathode emitter is 73.8 mm, its width is 1 mm. The suppressing electrodes are installed to suppress emission by the appropriate voltage, applied to the electrodes, which is necessary for efficient operation in a typical pulsed mode of injection. The gap between the annular emitter and the suppressing electrodes is 0.4 mm, the slit between the suppressing electrodes has radial width 1 mm. The cathode–anode gap corresponds to $d=10$ mm, it defines the electron scattering angle and gun

perveance. The chosen gun is an annular version of the Pierce-type on gun since the slopes of the focusing electrodes are 22.50 with the central magnetic flux line. The entrance anode diaphragm has a radial size of 4.5 mm that corresponds to an available aperture of the tubular string electrons in the ion confinement region of $h_{ap} = 1$ mm. The anode diaphragm provides collection of the string electrons that leave the system in the radial direction due to electron scattering and diffusion.

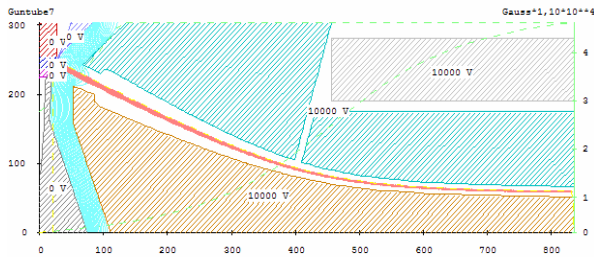


Figure 6 Formation of tubular electron beam in the fringe solenoid field.

The electron reflector was chosen to be mirror symmetrically with respect to the solenoid center. The orifice for ion extraction is foreseen to be arranged instead of the emitter at some azimuthal position of the reflector. The reflection voltage is chosen to be a few kV lower than the cathode voltage in order to ensure total reflection of the whole electron beam.

The drift tube structure (Figure7) consists of several electrodes which are used for production of ion traps, formation of a tubular ion beam (Figure7), off-axis ion extraction, and observation by means of pick-up electrodes of processes related to the electron string and ion beam formation. The ion extraction channel runs along the magnetic flux line at a definite azimuthal angle. Off-axis ion extraction was simulated with use of the Opera-3D code. On the basis of these simulations the azimuthal width of the extraction channel was optimally chosen to be 10^0 . The extraction channel begins in the uniform magnetic field region and consists of several electrodes which follow the shape and size of the corresponding magnetic flux lines up to B_{min} . Azimuthal ion migration in a uniform field region naturally occurs due to drift motion of ions in the longitudinal magnetic and radial electrical fields. When ions approach the beginning of the extraction channel, they are reflected back to the uniform field region by the applied positive voltage, except those ions which are captured in the extraction channel. Ions in the extraction channel are azimuthally confined due to the potential well created everywhere along the extraction channel in the azimuthal direction. Moreover, ions are accelerated towards the extraction orifice in the weak magnetic field due to the gradual decrease in the applied potentials along the extraction channel. It was proven in various simulations that ions could be accelerated to $2 \cdot Z$ keV in the extraction

channel without disturbing the electron beam. The electron reflector mounted at B_{min} reflects electrons and extracts ions. The extracted ion beam penetrates the orifice in the reflector placed at the same azimuthal position as the ion extraction channel. The extracted ion beam has an ellipsoidal shape with diameter $\Delta r_i = 2$ mm in the radial direction and diameter $\Delta y_i = 8$ mm in the azimuthal one. This azimuthal size is the minimal one allowed by the voltage applied to the extraction electrodes at the chosen azimuthal size of the extraction channel.

The simulated beam spot sizes permit to define the normalized radial ϵ_{r-n} and azimuthal $\epsilon_{\phi-n}$ emittances of the extracted ion beam: $\epsilon_{r-n} = \beta_i \cdot \Delta r_i^2 / 4 \rho_i = 0.04 \pi \cdot \text{mm} \cdot \text{mrad}$, $\epsilon_{\phi-n} \approx \beta_i \cdot \Delta r_i \cdot \Delta y_i / 4 \rho_i = 0.15 \pi \cdot \text{mm} \cdot \text{mrad}$, where $\beta_i = v_i / c = 3.5 \cdot 10^{-3}$, v_i is the velocity of extracted ions at reflector electrode voltage $U_{ref} = 6$ kV, $\rho_i = v_i / \omega_i = 10$ cm is the ion Larmor radius calculated at ion energy ZeU_{ref} , $2\rho_i$ plays a role of β -function, ω_i is the ion cyclotron frequency in the magnetic field B_{min} . We assume that the ion azimuthal angle spread is comparable with the radial one. The radial and azimuthal emittances of the extracted ion beam accelerated to energy of $eU_{ac} = 25 \cdot Z$ keV are $\epsilon_r \approx 5 \pi \cdot \text{mm} \cdot \text{mrad}$ and $\epsilon_{\phi} \approx 20 \pi \cdot \text{mm} \cdot \text{mrad}$.

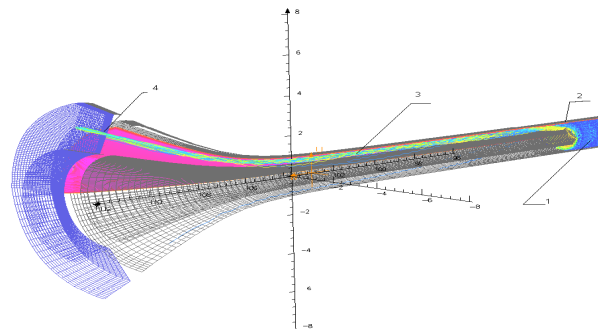


Figure 7. OPERA 3D simulation of the ion optic system and the ion off-axis extraction channel.

ACKNOWLEDGEMENTS

The research was supported by International Science and Technology Center, grant № 3454. Discussions with L. Liljeby and H. Danared are greatly acknowledged. E.E.D. is grateful to the Manne Siegbahn Laboratory (Stockholm, Sweden) for hospitality where numerical simulations with use of Opera-3D code were performed.

REFERENCES

- [1] E.D. Donets, Physica Scripta T12 (1996), p.11.
- [2]. E.D. Donets, Rev. Sci. Instrum. 71 (2000), p. 810.
- [3] E.D. Donets et al., Rev. Sci. Instr. 75 (2004), p. 1543.
- [4] E.D. Donets, et al., Rev. Sci. Instr. 73 (2002), p. 696.
- [5] E.E. Donets, J. of Phys.: Conf. Series 2, (2004) p. 97.
- [6] E.E. Donets et al, EPAC 08, (2008), p. 403.